REFERENCIAS BIBLIOGRAFICAS

1) A.E. Martell y R.D. Hancock, *Metal Complexes in Aqueous Solutions*, Editorial Plenum Press, New York, 1996. p63-120.

2) L. Stryer, *Biochemistry*, Segunda edición. Ed. W.H. Freeman and Company. New York, 1981. p431-453.

3) G.A. Melson, *Coordination Chemistry of Macrocyclic Compounds*, Editorial Plenum Press, New York, 1979. p1-6.

4) L.F. Linday, *The Chemistry of Macrocyclic Ligand Complexes*, Editorial Cambridge University Press, New York, 1989.

5) Y. A. Zolotov, *Macrocyclic Compounds in Analytical Chemistry*, Editorial John Wiley & Sons, Inc., New York, 1997. p41-62.

6) B.G. Cox y H. Schneider, *Coordination and Transport Properties of Macrocyclic Commpounds in Solution*, Editorial Elsevier Science Publishers. New York, 1992.

7) J. Rebek, Jr., "Model Studies in Molecular Recognition", Science 235 (1987) 1478-1483.

8) F. Diederich, "Molecular Recognition in Aqueous Solution", J. Chem. Educ. 67 (1990) 813-820.

9) H.J. Schneider, "Mechanisms of Molecular Recognition: Investigation of Organic Host-Guest Complexes", Angew. Chem. Int. Ed. Engl. 30 (1991) 1417-1436.

10) S.H. Gellman, "Introduction: Molecular Recognition", Chem. Rev. 97 (1997) 1231-1232.

11) A.D. Hamilton, "Molecular Recognition. Design and Synthesis of Artificial Receptors Employing Directed Hydrogen Bonding Interactions", J. Chem. Educ. 67 (1990) 821-828.

12) J.M. Lehn, "Supramolecular Chemistry - Scope and Perspectives. Molecules, Supermolecules, and Molecular Devices", Angew. Chem. Int. Ed. Engl. 27 (1988) 89-112.

13) J.M. Lehn, *Supramolecular Chemistry. Concepts and Perspectives*, Editorial VCH, Alemania, 1995. p11-30.

14) E.J. Baran, *Química Bioinorgánica*, Editorial McGraw-Hill/Interamericana, Madrid, 1995. p19-27.

15) H. Dugas, *Bioorganic Chemistry. A Chemical Approach to Enzyme Action*, Editorial Springer, New York, 3ª edición, 1996. p252-387.

16) D.K. Cabbiness y D.W. Margerum, "Macrocyclic Effect on the Stability of Copper(II) Tetramine Complexes" J.Am.Chem.Soc. 91:23 (1969) 6540.

17) F. Diederich, "Cyclophanes". Editorial The Royal Society of Chemistry, Cambridge, 1991. p1-3.

18) D.J. Cram, "The Design of Molecular Host, Guest and their Complexes", Angew. Chem. Int. Ed. Engl. 27 (1988) 1009 - 1020.

19) F.A. Cotton, G. Wilikinson, C.A. Murillo y M. Bochman. *Advanced Inorganic Chemistry*. Sexta edición. Ed. John Wiley & sons Inc. E.U.A. 1999 p85-89.

20) D.J. Cram, H. Steinberg, *J.Am. Chem.Soc.*, 1951, **73**, 5691.

21) K. Odashima y K. Koga, "Cyclophanes in Host-Guest Chemistry" en *Cyclophanes, Vol II*, Editorial Academic Press, Inc., 1983, p629 - 677.

22) P. Mattei y F. Diederich, "A Flavo-Thiazolio-Ciclophane as a Functional Model for Pyruvate Oxidase" Angew. Chem. Int. Ed. Engl, **35**, (1996) 1341-1344.

23) D.F. Shriver, P. Atkins y C.H. Lanfgord, *Inorganic Chemistry*, segunda edición. Editorial W.H. Freeman and Company, New York, 1994. p226-266, 581-601.

24) R. Chang, *Chemistry*. Tercera edición. Editorial Random House, NewYork, 1988. p909-941.

25) G.E. Rodgers, *Química Inorgánica. Introducción a la Química de Coordinación del Estado Sólido y Descriptiva* Editorial McGraw Hill, España, 1995. p11-32.

26) M.Gerloch y E.C. Constable, *Transition Metal Chemistry. The Valence Shell in d-Block Chemistry*. Editorial VCH, Alemania, 1994. p40-56, 161-165.

27) G. L. Miessler, D.A.Tarr, "Inorganic Chemistry" Segunda edición. Ed. Prentice Hall. New Jersey, 1999. p352.

28) M.B. Inoue, M. Inoue, R. Sugich, L.Machi, E.F. Velázquez y Q. Fernando. "High Steric Constraints and Molecular Distortion in Methyl-Substituted Amide-Based Paracyclophanes and the Binuclear Cu^{2+} Complexes: X-ray Structures, NMR, Luminescence and Absorption Spectra" Inorg. Chim. Acta, 317 (2001) 181-189.

29) M.B. Inoue, I.C. Muñoz, L.Machi, M. Inoue, Q. Fernando, "Structural and Spectroscopic Studies of Binuclear Cu^{2+} and Co^{2+} Complexes with an Amide-Based Naphtalenophane" Inorg. Chim. Acta. 311 (2000) 50-56.

30) M.B. Inoue, E.F. Velázquez, F. Medrano, K.L. Ochoa, J.C.Gálvez, M. Inoue, Q. Fernando. "Binuclear Copper(II) Chelates of Amide Based Cyclophanes" Inorg. Chem. 37 (1998) 4070-4075.

31) M.B. Inoue, E.F. Velázquez, M. Inoue, Q. Fernando, "Molecular Recognition of Phenetylamine, Tyramine and Dopamine with New Anionic Cyclophanes in Aqueous Media". T. Chem. Soc. Perkin Trans. 2 (1997) 2113-2118.

32) D.J. Cram, N.L. Allinger, H. Steinberg, "Macro rings. VII. The Spectral Consequences of Bringing Two Benzene Rings Face to Face", J.Am.Chem.Soc. 76 (1954) 6132-6141.

33) D.J. Cram, R.H.Bauer, "Macro rings. XX. Transannular Effects in π - π Complexes", J.Am.Chem.Soc. 81(1959) 5971-5977.

34) D.J. Cram, R.H. Bauer, N.L.Allinger, R.A. Reeves, W.J. Wechter, E. Heilbronner. "Macro Rings. XXI. Mono- and Polysubstituted [2.2]paracyclophanes" J.Am.Chem.Soc. 81 (1959) 5977-5983.

ELSEVIER

www.elsevier.nl/locate/ica

Inorganica Chimica Acta 317 (2001) 181–189

Inorganica Chimica Acta

High steric constraints and molecular distortion in methyl-substituted amide-based paracyclophanes and the binuclear Cu^{2+} complexes: X-ray structures, NMR and absorption spectra

Michiko B. Inoue [a,b,*], Motomichi Inoue [b], Rocio Sugich-Miranda [b], Lorena Machi [b], Enrique F. Velazquez [b], Quintus Fernando [a]

[a] *Department of Chemistry, University of Arizona, Tucson, AZ 85721-0041, USA*
[b] *CIPM, Universidad de Sonora, Hermosillo, Sonora 83000, Mexico*

Received 31 October 2000; accepted 31 January 2001

Abstract

Chelating paracyclophanes that are sterically constrained to a great extent have been synthesized and characterized by X-ray crystallography and NMR spectroscopy: the macrocycles studied are 2,9,18,25-tetraoxo-4,7,20,23-tetrakis(carboxymethyl)-1,4,7,10,17,20,23,26-octaaza[10.10]paracyclophane, abbreviated as (Lpd)H_4, and its 2,5-dimethyl-*p*-phenylene and tetramethyl-*p*-phenylene derivatives, abbreviated as (Ldmpd)H_4 and (Ltmpd)H_4, respectively. Steric interaction between tetramethylphenylene and amide groups in the tetramethyl derivative defines the conformation of the macrocyclic cavity, and causes unusual spectroscopic and chemical properties including the extreme line-broadening of ^{1}H NMR signals and the low basicity of amino nitrogen; such properties are not observed for the other macrocycles, in which steric interaction between phenylene and amide groups is less effective. The complexation of the highly strained ligand (Ltmpd)H_4 with Cu^{2+} ions has been studied by X-ray crystallography and solution electronic spectroscopy. The macrocycle forms a binuclear complex of $[Cu_2(LH_{-4})]^{4-}$ type in which four amide nitrogen atoms are deprotonated and each metal ion is coordinated to two amide nitrogen atoms and two amino nitrogen atoms. In the binuclear chelate molecule, the severe contraction of the macrocyclic ring forces the phenylene groups distorted to a boat form, due to the steric effect of the tetramethyl substituents. As a result, the metal–ligand charge-transfer interaction in the binuclear complex differs from that in the mononuclear chelate of the same macrocycle.

Keywords: Crystal structures; Copper complexes; Macrocyclic complexes; Binuclear complexes

1. Introduction

Preorganization of ligand molecules is a major strategy for the molecular design of receptors that have a high molecular recognition capability toward specific metal ions [1–7]. When a macrocyclic ligand is protonated or coordinated to a metal ion, the conformation of the ligand molecule is altered. When such a conformational change is obstructed by the introduction of bulky groups into a macrocyclic ligand, the resulting macrocycle will show complexation properties that differ from those of the parent macrocycle, even when the electron densities on the donor atoms are not influenced by the introduced groups. This is an approach to the preorganization of macrocycles. This paper reports a novel example in which macrocycles that have an identical ring size and an identical arrangement of donor atoms show different acidities, spectroscopic properties and coordination properties due to a difference in steric effects.

Reactions between ethylenediaminetetraacetic (edta) dianhydride and aromatic diamines (such as *p*-phenylenediamine) provide a series of amide-based chelating paracyclophanes represented by macrocycle **1** (Fig. 1) in which two edta units and two diamine units are linked by amide bonds [8–10]; macrocycle **1** is

* Corresponding author. Tel.: +1-520-621 6340; fax: +1-520-621 8407.
E-mail address: minoue@u.arizona.edu (M.B. Inoue).

0020-1693/01/$ - see front matter
PII: S0020-1693(01)00362-0

abbreviated as (Lpd)H_4 that indicates the diamine unit and the number of acidic protons. If the conformational change of the ligand upon metal complexation can be hindered by the introduction of bulky groups into the phenylene groups of (Lpd)H_4, the resulting macrocycle will be ideal for studying the steric effect on metal complexation, because the substituent groups do not directly influence the electron density and consequently electron-donating capability of the donor atoms. On the basis of this presumption, we have synthesized dimethyl and tetramethyl derivatives, (Ldmpd)H_4 (**2** in Fig. 1) and (Ltmpd)H_4 (**3** in Fig. 1), and studied their solid state structures and solution properties related to molecular motion. For studying the steric effect on metal complexation, Cu^{2+} is the best central metal because the Cu^{2+} complex of the amide-based cyclophane is expected to show a structural conversion between structures **A** and **B** in Fig. 1 depending on pH, as reported for the Cu^{2+} complexes of (Lpd)H_4 [10,11]. The solution electronic spectra and X-ray structure of the binuclear Cu^{2+} complex of the tetramethyl derivative **3** have shown the formation of a highly strained metal chelate molecule as a result of a steric interaction between tetramethyl-*p*-phenylene and amide groups.

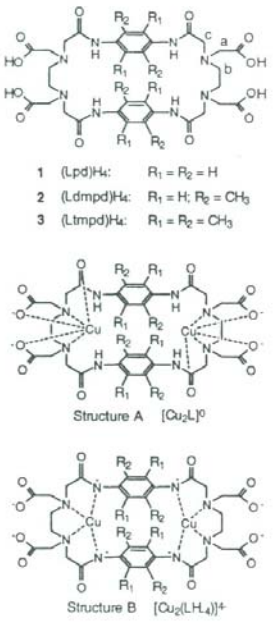

Fig. 1. Chelating paracyclophanes studied and the possible structures of the binuclear Cu^{2+} chelates.

2. Experimental

2.1. Syntheses of macrocycles

Macrocycle **1**, (Lpd)H_4, was synthesized by a reaction between ethylenediaminetetraacetic (edta) dianhydride (Aldrich) and *p*-phenylenediamine (Aldrich 97% grade) by the method reported previously [10]. A similar method was used for the synthesis of (Ltmpd)H_4. 2,3,5,6-Tetramethyl-*p*-phenylenediamine (2.1 g, Aldrich 97% grade) dissolved in dry dimethylformamide (DMF, 90 ml) was added dropwise in a period of 4 h to edta dianhydride (3.0 g) suspended in DMF (200 ml) with vigorous stirring under a nitrogen atmosphere. After the resulting mixture was stirred overnight, any solid formed was removed by filtration. The filtrate was concentrated to an oil, to which ethanol (30 ml) was added. The solid formed was collected by filtration. The solid obtained was suspended in water (40 ml). To the suspension, solid Li_2CO_3 was added little by little until a clear solution was obtained. The resulting solution (pH $\approx$ 7.5) was concentrated to half the initial volume, to which ethanol (20 ml) was added. The solid formed was collected by filtration and dried in vacuum, and then washed by suspending in methanol (20 ml) overnight. The solid separated was mixed with a small amount of water so as to form a mull, which was dissolved by adding methanol. Concentration of the resulting methanol solution gave the product as its lithium salt. When an aqueous solution of the lithium salt was acidified with dilute HCl until the pH was approximately 2, the product was obtained in the acid form, and was collected by filtration, successively washed by suspending in water, collected by filtration again and dried in vacuum. Yield: 10%. *Anal.* Found: C, 52.23; H, 6.93; N, 12.03. Calc. for $C_{40}H_{56}N_8O_{12}\cdot 4H_2O$: C, 52.62; H, 7.07; N, 12.27%. ^{1}H NMR (H_2O-d_2/Na_2CO_3, pD 10.2, DSS): $\delta = 1.85$ (s, 24H, assigned to CH_3), 2.94 (s, 8H, H*b* in Fig. 1); 3.33 (s, 8H, H*a*); 3.42 (s, 8H, H*c*). ^{13}C NMR (H_2O-d_2/KOH-d, pD 10.6, DSS): $\delta = 17.29$ (methyl); 55.97 (C*b*); 61.10, 62.27 (C*a*, C*c*); 134.76, 134.99 (phenylene C–N, C–Me); 176.94 (CONH); 181.89 (CO_2^-). Mass spectrum (ESI): $m/z = 839.7$ ($[M-H]^-$, 100%); 419.6 ($[M-2H]^{2-}$, 32%).

The use of 2,5-dimethyl-*p*-phenylenediamine (Aldrich 97% grade) as the diamine source gave (Ldmpd)H_4. The process of purification was similar to that for (Ltmpd)H_4. Yield: 8%. *Anal.* Found: C, 53.74; H, 5.68; N, 13.76. Calc. for $C_{36}H_{48}N_8O_{12}\cdot H_2O$: C, 53.86; H, 6.28; N, 13.95%. ^{1}H NMR (H_2O-d_2/Na_2CO_3, pD 10.6, DSS): $\delta = 1.96$ (s, 12H, CH_3); 2.88 (s, 8H, H*b*); 3.29 (s, 8H, H*a*); 3.44 (s, 8H, H*c*); 6.98 (s, 4H, phenylene H). ^{13}C NMR (H_2O-d_2/KOH-d, pD 11.8, DSS): $\delta = 19.29$ (methyl); 55.54 (C*b*); 60.88, 61.39 (C*a*, C*c*); 129.80 (phenylene C–H); 133.64, 134.70 (phenylene C–N,

Table 1
Crystallographic data for Li_2H_2(Ltmpd)·$10H_2O$, 3(Lpd)H_4·$2HCl$·$24H_2O$, and $K_4[Cu_2(LtmpdH_{-4})]$·$11H_2O$

	Li_2H_2(Ltmpd)·$10H_2O$	3(Lpd)H_4·$2HCl$·$24H_2O$	$K_4[Cu_2(LtmpdH_{-4})]$·$11H_2O$
Chemical formula	$Li_2C_{40}H_{54}N_8O_{12}·10H_2O$	$C_{96}H_{122}N_{24}O_{36}Cl_2·24H_2O$	$K_4Cu_2C_{40}H_{48}N_8O_{12}·11H_2O$
Temperature (K)	170	300	170
Space group	$P\bar{1}$ (No. 2)	$P\bar{1}$ (No. 2)	$P2_1/n$ (No. 14)
Unit cell dimensions			
a (Å)	8.689(1)	13.4431(5)	12.664(1)
b (Å)	8.728(1)	14.8469(6)	14.789(1)
c (Å)	18.993(4)	17.4663(7)	15.707(1)
α (°)	102.25(1)	71.494(1)	90
β (°)	90.48(2)	85.056(1)	94.431(2)
γ (°)	108.98(2)	83.448(1)	90
V (Å^3)	1326.4(4)	3279.6(2)	2932.8(4)
Z	1	1	2
ρ_{calc} (Mg m^{-3})	1.293	1.363	1.489
μ (mm^{-1})	0.104	0.152	1.089
R_1/wR_2 [$I>2\sigma(I)$] [a]	0.0635/0.1357	0.0793/0.2127	0.0847/0.2248

[a] $R_1 = \Sigma||F_o|-|F_c||/\Sigma|F_o|$; $wR2 = \{\Sigma[w(F_o^2-F_c^2)^2]/\Sigma[w(F_o^2)^2]\}^{1/2}$; $w = 1/[\sigma^2(F_o^2)+(aP)^2+bP]$, $P = [2F_c^2+\max(F_o^2,0)]/3$; $a = 0.0651$ and $b = 0$ for Li_2H_2(Ltmpd)·$10H_2O$; $a = 0.1$ and $b = 0$ for 3(Lpd)H_4·$2HCl$·$24H_2O$; $a = 0.1$ and $b = 12.0$ for $K_4[Cu_2(LtmpdH_{-4})]$·$11H_2O$.

C–Me); 176.36 (CONH); 181.80 (CO_2^-). Mass spectrum (ESI): m/z 783.2 ([M − H]$^-$, 100%).

2.2. X-ray crystal analyses

Diffraction data were collected with graphite-monochromated Mo Kα radiation ($\lambda = 0.71073$ Å) on a Bruker SMART 1000 X-ray diffractometer equipped with a CCD area detector. Data processing was carried out with the software package Bruker SAINT version 6.01, and structure determination was performed by the use of a Bruker SHELXTL version 5.1 software package. The scattering factors were taken from the International Tables for Crystallography, Vol. C, Table 6.1.1.4. The crystallographic data are summarized in Table 1.

Single crystals of $Li_2[(Ltmpd)H_2]·10H_2O$ were obtained by diffusing ethanol into an aqueous solution that was prepared by adding a minimum amount of solid Li_2CO_3 to a suspension of the macrocycle in a small amount of water in a small-bore tube. A colorless plate-like crystal with approximate dimensions of $0.03 \times 0.10 \times 0.25$ mm^3 was mounted on a glass fiber with an inert oil and transferred to a cold nitrogen stream of the diffractometer. The data collection was performed at a temperature of 170 K: $0 < 2\theta < 56.3°$; total reflections ($\pm h$, $\pm k$, $\pm l$) = 15 097; unique reflections = 5884. The structure was solved by direct methods followed by Fourier syntheses. Hydrogen atoms were added at idealized positions for the ligand molecule and at peak positions for water molecules, and they were constrained to ride on the atoms to which they are bonded.

Single crystals of 3[(Lpd)H_4]·$2HCl$·$24H_2O$ were grown by diffusing HCl vapor into an aqueous solution that was prepared by adding solid Na_2CO_3 to a suspension of the ligand in a small amount of water (pH ≈ 8). The crystals were highly efflorescent. A prismatic crystal with approximate dimensions of $0.17 \times 0.20 \times 0.47$ mm^3 was sealed in a glass capillary together with the mother liquor, and the data collection was carried out at 300 K: $0 < 2\theta < 50°$; total reflections ($\pm h$, $\pm k$, $\pm l$) = 17 748; unique reflections = 11 486. Carbon and oxygen atoms in a carboxylate group and two water molecules were disordered. Hydrogen atoms were included in the refinement in the same manner as for $Li_2[(Ltmpd)H_2]·10H_2O$, but the hydrogen atoms of most solvent molecules were excluded.

Single crystals of $K_4[Cu_2(LtmpdH_{-4})]·11H_2O$ in which four amide nitrogen atoms are deprotonated were obtained as follows. When excess $CuCl_2$ was added to an aqueous solution of the lithium salt of the ligand, a pale blue solid formed immediately. The product was dissolved in a small amount of 0.1 M KOH in a small-bore tube. Ethanol was added to the surface of the resulting deep brownish green solution. After the interface between the two liquid layers disappeared in a week, acetone was diffused into the resulting solution. Deep blue green crystals were obtained in a few weeks. A plate-like crystal with approximate dimensions of $0.05 \times 0.18 \times 0.43$ mm^3 was sealed in a glass capillary together with the mother liquor; the crystal was highly efflorescent. The data collection was performed at 170 K: $0 < 2\theta < 50°$; total reflections ($\pm h$, $\pm k$, $\pm l$) = 28 421; unique reflections = 5158. Empirical absorption corrections were applied by using the program SADABS: $T_{min} = 0.553$ and $T_{max} = 0.969$. The crystal contained disordered water molecules that were readily liberated. Some of the water molecules were disordered in several positions. These molecules

were refined isotropically, and their occupancies were determined in such a manner that their displacement parameters were almost identical.

2.3. Spectroscopic measurements

The NMR spectra were obtained with a Bruker AM 250 spectrometer for H_2O-d_2 solutions at a probe temperature of approximately 23°C. The internal reference was sodium 2,2-dimethyl-2-silapentane-5-sulfonate (DSS). A minimum quantity of dilute KOH-d solution or dilute DCl was used for adjusting the pD of the sample solutions. The pH value of each sample solution was measured with a long-stem combination electrode inserted into the NMR sample tube after NMR experiments. The electrode was calibrated with standard aqueous buffers, and the measured pH values were converted to pD values by the relation $pD = pH_{measd} + 0.44$ [12,13]. Solution electronic spectra were recorded on a Perkin–Elmer Lambda 2 UV–Vis spectrometer. The ligands were dissolved in 0.01 M NaCl solution by adding an equimolar amount of solid Na_2CO_3; the water solubilities of the macrocycles markedly decreased with decreasing pH at $pH < 7$. The pH values of sample solutions were adjusted by using 0.01 M HCl and 0.01 M NaOH so that the ionic strength was kept constant. Sample solutions of the Cu^{2+} complexes were prepared from stock solutions of $CuCl_2$ and the appropriate ligands. The mass spectra were obtained by the use of a JEOL HX 110A spectrometer.

3. Results and discussion

3.1. X-ray structures of the macrocycles

Fig. 2 shows the molecular structure of $[Li(H_2O)_3]_2^+$-$[(Ltmpd)H_2]^{2-}$. An electron-density peak assignable to H was located at a position close to N(3) with a distance of 0.95 Å reasonable for an N–H bond, whereas no peak was visible near N(2). Thus, the protonated amino nitrogen was unequivocally identified to be N(3). The protonated amino nitrogen N(3) forms an intramolecular hydrogen bond with O(2) in the other $>NCH_2CO_2^-$ unit that is not protonated at its nitrogen or oxygen atom. The molecular planes of the two phenylene rings in a molecule are parallel to each other with a face-to-face distance of 4.417(3) Å, the closest C–C distance being 4.250(4) Å for C(12)–C(19)′. These distances are much longer than the van der Waals contact (3.4 Å) predicted for the face-to-face stack of aromatic molecules and still longer than the C–C distance 4.0 Å predicted for the van der Waals contact of methyl groups [14]. The least-squares planes of the amide groups are rotated by 59.77(10) and 67.12(8)° from the phenylene ring plane due to the steric effect of methyl groups. This steric effect between the methyl and amide groups results in (1) the long intramolecular face-to-face distance between the phen-

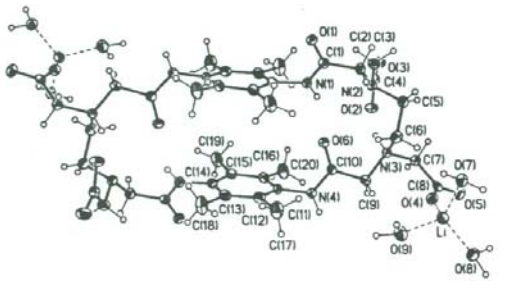

Fig. 2. Molecular structure of $[Li(H_2O)_3]_2[(Ltmpd)H_2]$. The molecule has an inversion center. The atoms are shown at the 50% probability level. Intramolecular hydrogen bonds: $d[N(1)\cdots O(6)] = 2.848(3)$ Å, $\angle[N(1)-H\cdots O(6)] = 148.1°$; $d[N(3)\cdots O(2)] = 2.750(2)$ Å, $\angle[N(3)-H\cdots O(2)] = 149.0°$.

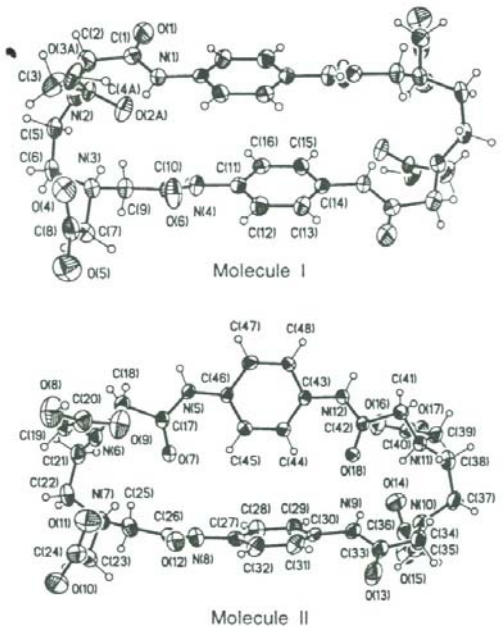

Fig. 3. Structures of molecule I (top), $[(Lpd)H_4]^0$, and molecule II (bottom), $[(Lpd)H_5]^+$, involved in $3(Lpd)H_4{\cdot}2HCl{\cdot}24H_2O$. The atoms are shown at the 30% probability level. Molecule I has an inversion center. Atoms C(4), O(2) and O(3) in a carboxylate group in molecule I are disordered at two positions; only one (labeled A) of the positions is shown for each atom for clarity. Hydrogen bonds: in molecule I, $d[N(1)\cdots O(2A)] = 2.759(11)$ Å, $\angle[N(1)-H\cdots O(2A)] = 149.5°$; in molecule II, $d[N(9)\cdots O(18)] = 2.944(5)$ Å, $\angle[N(9)-H\cdots O(18)] = 138.1°$.

Table 2
Geometrical parameters related to paraphenylene groups in $[(Ltmpd)H_2]^{2-}$, $[Cu_2(LtmpdH_{-4})]^{4-}$, $[(Lpd)H_4]^0$ and $[(Lpd)H_5]^+$

	$[(Ltmpd)H_2]^{2-}$	$[Cu_2(LtmpdH_{-4})]^{4-}$		$[(Lpd)H_4]^0$	$[(Lpd)H_5]^+$	
Deviations (Å) of atoms from the least-squares plane of the *p*-phenylene ring [a]						
$C(11)_{para}$	0.007(2)	0.031(5)	0.047(11) [b]	<0.01	C(27)	<0.01
$C(14)_{para}$	0.017(2)	0.030(5)	0.045(11) [b]	<0.01	C(30)	<0.01
$N(1)_{amide}$	0.109(3)	0.086(10)	0.100(16) [b]	−0.010(6)	N(5)	0.077(6)
$N(4)_{amide}$	0.053(3)	0.129(10)	0.146(16) [b]	0.037(6)	N(12)	0.077(6)
$C(17)_{Me}$	−0.060(4)	−0.104(13)	−0.087(14) [b]		N(8)	0.112(7)
$C(18)_{Me}$	0.021(4)	−0.100(13)	−0.085(15) [b]		N(9)	0.042(7)
$C(19)_{Me}$	−0.170(4)	−0.058(13)	−0.044(15) [b]			
$C(20)_{Me}$	0.126(4)	−0.137(13)	−0.121(15) [b]			
Distances (Å) between the least-squares planes of two *p*-phenylene rings in a molecule						
	4.417(3)	3.411(8)	3.442(8) [c]	3.432(5)	edge-to-face	
Angles (°) between the amide and phenylene ring planes						
	59.77(10)	86.5(3)		11.7(4)	12.3(2)	28.9(3)
	67.12(8)	87.8(3)		26.4(2)	3.6(4)	9.3(3)

[a] The positive sign indicates deviation toward the other *p*-phenylene ring in the same molecule, and the negative sign indicates deviation to the opposite direction; for N(5) and N(12) bonded to the edge-stacked phenylene ring in $[(Lpd)H_5]^+$, the sign of deviation is not defined.

[b] Deviations from the least-squares plane of four carbon atoms C(12), C(13), C(15) and C(16) which are in the plane within a deviation of 0.004 Å; the phenylene ring is distorted in a boat form with dihedral angles, 3.7–3.9°.

[c] Distance of the least-squares plane of four ring carbon atoms, C(12), C(13), C(15) and C(16), from the corresponding plane of the other *p*-phenylene group that faces the former.

ylene rings, and (2) the deviation of methyl carbon atoms C(19) and C(20) from the phenylene plane (Table 2). The effects of the methyl substituents are verified by comparison with the X-ray structure of the unsubstituted cyclophane, $(Lpd)H_4$.

The unit cell of $3[(Lpd)H_4]\cdot 2HCl\cdot 24H_2O$ contains three macrocyclic molecules, two of which are crystallographically equivalent. One molecule, labeled I in Fig. 3, has an inversion center and half the molecule is unique, whereas two crystallographically equivalent molecules, labeled II, are asymmetric. The protonated nitrogen atom in molecule I is identified to be N(3) by the same method as for $[(Ltmpd)H_2]^{2-}$. A hydrogen peak was located at a position of O(3A)–H = 1.15 Å, and the C(4A)–O(3A) distance is approximately 0.1 Å longer than C(4A)–O(2A), whereas in the carboxylate group C(8)O(4)O(5), two C–O distances are ≈1.25 Å and their difference is not larger than 0.03 Å. These observations show that the carboxylate oxygen atom O(3) is protonated. Molecule I, therefore, can be formulated as $[(Lpd)H_4]^0$, in which two *N*-carboxymethyl groups have the dipolar (or zwitterion) form, $>NH^+CH_2CO_2^-$, and the other two have the neutral form $>NCH_2CO_2H$. The protonated donor atoms in molecule II are identified to be N(7), N(11), O(8), O(15) and O(17) on the basis of the same criteria as for molecule I. Molecule II is, therefore, formulated as $[(Lpd)H_5]^+$ in which three types of *N*-carboxymethyl groups are involved: an $>NH^+CH_2CO_2^-$ group, two $>NCH_2CO_2H$ groups, and an $>NH^+CH_2CO_2H$ group. A counter-anion Cl^- is located at a position apart by 3.114(4) Å from the amide nitrogen N(12), and these atoms are connected by a hydrogen bond. The composition of the crystal studied is, therefore, described by $[(Lpd)H_4]^0\cdot[(Lpd)H_5^+Cl^-]_2$.

Molecule I, $[(Lpd)H_4]^0$, contains a slipped face-to-face contact with an interfacial distance of 3.432(5) Å, which is nearly equal to the value, 3.4 Å, predicted for the van der Waals contact of aromatic molecules. In molecule II, $[(Lpd)H_5]^+$, the phenylene groups form an edge-to-face contact. Electrostatic interaction between two phenylene groups stabilizes an edge-to-face contact, and a face-to-face stack is stable only in the slipped form [15]. Both types of contacts are formed in this crystal. The molecular planes of amide groups in molecules I and II are rotated by 4–29° from the planes of the phenylene groups to which they are bonded (Table 2); the π-electron systems of the amide groups are conjugated with the phenyl groups, whereas such a conjugation is absent in the tetramethyl derivative. Thus, the introduction of methyl groups in the aromatic groups results in the different conformations of the macrocycles, which may be an important controlling factor of metal complexation.

3.2. ^1H NMR spectra and protonation of the macrocycles in solution

Fig. 4 shows the ^1H NMR spectra of $(Ltmpd)H_4$ at different pD values, and the chemical shift and the full width at half maximum (fwhm) of each signal are plotted in Fig. 5 as functions of pD. At pD > 9 four sharp peaks were observed, and hence four subunits in a molecule are chemically equivalent due to rapid inter-

nal fluctuation. All signals shifted downfield with decreasing pD at pD < 9. Simultaneously the linewidths of the signals increased extraordinarily, except for the methyl proton signal; at pD < 8 only the methyl protons showed a well-defined signal. Such an extreme line-broadening in ^{1}H NMR spectra was not observed for (Lpd)H_4 and (Ldmpd)H_4.

The chemical shift of the ith CH_2 proton ($i = a$, b, etc. in Fig. 1) in $(Lpd)^{4-}$ and $(Ldmpd)^{4-}$ can be explained by the following function of pD (Fig. 6):

$$\delta_i(\mathrm{pD}) = \{\delta_{i,0} + \Sigma_n \delta_{i,n}\beta_n 10^{-n(\mathrm{pD})}\}/\{1 + \Sigma_n \beta_n 10^{-n(\mathrm{pD})}\} \quad (1)$$

Here β_n is the overall protonation constant at the nth protonation step, $\delta_{i,0}$ is the chemical shift of the ith CH_2 proton in the completely deprotonated species shown by the general formula L^{4-}, and $\delta_{i,n}$ the chemical shift of the ith proton in the species formed at the nth protonation step. Simulation curves obtained on the basis of Eq. (1) are shown by the solid lines in Fig. 6; the parameters for the best fits are given in the caption. For (Ltmpd)H_4, simulation can be performed only for the methyl group; other proton signals are extremely broad, and hence the simulation curves are shown tentatively by the use of the β_1 value obtained from the methyl proton signal. The increase in the $\delta_{i,n}$ value, $\delta_{i,n} - \delta_{i,n-1}$, at the nth protonation step is related to an increase in proton population on the adjacent donor atom at the corresponding protonation step [16,17]. The large simultaneous changes in $\delta_{i,n}$ of all CH_2 proton signals in the pD region of 7–9 indicate that the protonation in this pD region occurs predominantly at amino nitrogen atoms; the next protonation at pD < 6 occurs at carboxylate oxygen atoms. The ^{1}H NMR spectra show that two edta units are equivalent

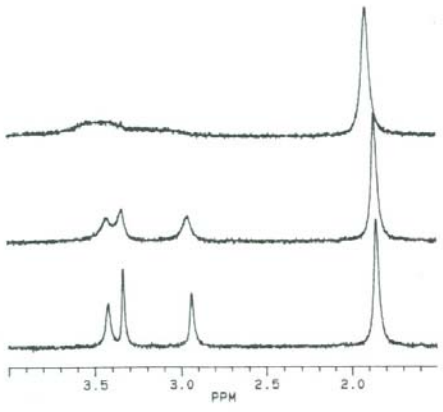

Fig. 4. ^{1}H NMR spectra of (Ltmpd)H_4 at pD 10.4 (bottom), 8.3 (middle) and 7.5 (top). Concentration = 5 mM; internal reference = DSS; temperature ≈ 23°C.

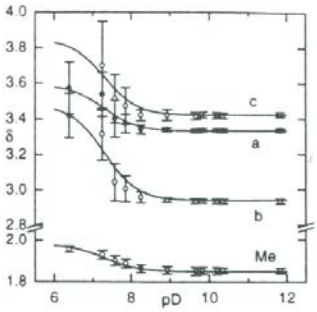

Fig. 5. ^{1}H NMR shifts δ (referenced to DSS) vs. pD observed for (Ltmpd)H_4; for labeling see Fig. 1. The vertical lines of the data points indicate the FWHM values of the signals. The solid lines are calculated by Eq. (1) with log $\beta_1 = 7.30$; $\delta_{Me,0} = 1.85$, $\delta_{Me,1} = 1.98$; $\delta_{a,0} = 3.33$, $\delta_{a,1} = 3.59$; $\delta_{b,0} = 2.94$, $\delta_{b,1} = 3.48$; $\delta_{c,0} = 3.42$, $\delta_{c,1} = 3.85$.

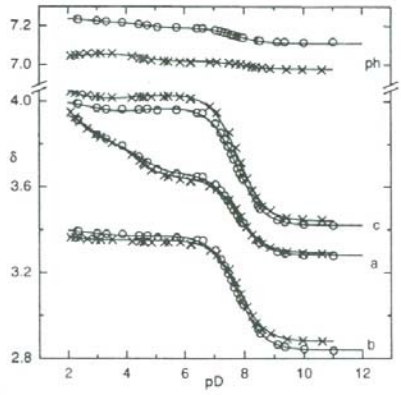

Fig. 6. ^{1}H NMR shifts δ (referenced to DSS) vs. pD observed for (Lpd)H_4 (○) and (Ldmpd)H_4 (×); for labeling see Fig. 1. The δ of the methyl proton signal of (Ldmpd)H_4 is not included. The solid lines are simulation curves obtained from Eq. (1) with the following values of the parameters: for $(Lpd)^{4-}$, log $\beta_1 = 7.77$, log $\beta_2 = 12.29$, log $\beta_3 = 15.01$, $\delta_{a,0} = 3.28$, $\delta_{a,1} = 3.66$, $\delta_{a,2} = 3.80$, $\delta_{a,3} = 3.96$, $\delta_{b,0} = 2.84$, $\delta_{b,1} = 3.37$, $\delta_{b,2} = 3.37$, $\delta_{b,3} = 3.40$, $\delta_{c,0} = 3.42$, $\delta_{c,1} = 3.97$, $\delta_{c,2} = 3.95$, $\delta_{c,3} = 4.00$, $\delta_{d,0} = 7.11$, $\delta_{d,1} = 7.19$, $\delta_{d,2} = 7.22$, $\delta_{d,3} = 7.24$; for (Ldmpd)H_4, log $\beta_1 = 7.82$, log $\beta_2 = 12.18$, log $\beta_3 = 14.25$, $\delta_{a,0} = 3.29$, $\delta_{a,1} = 3.64$, $\delta_{a,2} = 3.82$, $\delta_{a,3} = 4.09$, $\delta_{b,0} = 2.88$, $\delta_{b,1} = 3.35$, $\delta_{b,2} = 3.35$, $\delta_{b,3} = 3.37$, $\delta_{c,0} = 3.44$, $\delta_{c,1} = 4.03$, $\delta_{c,2} = 4.01$, $\delta_{c,3} = 4.08$, $\delta_{ph,0} = 6.98$, $\delta_{ph,1} = 7.02$, $\delta_{ph,2} = 7.06$, $\delta_{ph,3} = 7.02$, the parameters for the methyl protons, $\delta_{Me,0} = 1.96$, $\delta_{Me,1} = 2.06$, $\delta_{Me,2} = 2.05$, $\delta_{Me,3} = 2.05$.

in solution throughout the pD range studied. Protonation in two edta subunits occurs simultaneously in an independent manner; $[LH_2]^{2-}$ forms at the first protonation step and $[LH_4]^0$ at the second protonation step. Since all the N-carboxymethyl groups in the $[LH_2]^{2-}$ species are equivalent in solution, each acidic proton in $[LH_2]^{2-}$ is shared by two amino nitrogen atoms in each

$>NCH_2CH_2N<$ unit, and synchronously with this prototropy the internal molecular motion occurs. This internal motion in $[(Lpd)H_2]^{2-}$ and $[(Ldmpd)H_2]^{2-}$ is so fast that sharp ^1H NMR signals are observed throughout the pD range studied. In contrast, the internal molecular motion in $[(Ltmpd)H_2]^{2-}$ is hindered by the steric effect between the amide and tetramethylphenylene groups, and hence so sluggish as to result in the extremely broad ^1H NMR signals.

The β_n values determined from the ^1H NMR signals of a weak acid indicate the basicities of the donor atoms in H_2O-d_2 media. The log β_1 value, 7.30, determined for $(Ltmpd)^{4-}$ on the basis of the methyl proton signal is significantly smaller than the corresponding value 7.82 of $(Ldmpd)^{4-}$ and 7.77 of $(Lpd)^{4-}$; the estimated uncertainty in the curve fitting was ± 0.02, which was smaller than the uncertainty ± 0.03 of the conversion of pH_{meas} to pD [13]. The lower basicity of the amino nitrogen atoms in $(Ltmpd)^{4-}$ can also be interpreted by the steric effect of the tetramethylphenylene groups, as follows. The protonated state of a weak acid is stabilized when an acidic proton is shared by two electron-donor sites, and this stabilization increases the basicity of the donor site. Such a stabilization is less effective in $[(Ltmpd)H_2]^{2-}$, because the molecular reorientation accompanying proton exchange is hindered as shown by the line-broadening in the NMR spectrum. The tetramethyl substituents are too distant from the amino nitrogen atoms to influence the electron density on the donor atoms, but the steric effect of the methyl and amide groups decreases the basicity of the amino nitrogen in $(Ltmpd)^{4-}$.

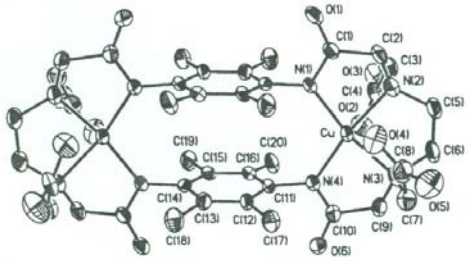

Fig. 7. Molecular structure of $[Cu_2(LtmpdH_{-4})]^{4-}$. The molecule has an inversion center. The atoms are shown at the 50% portability level. The M–X distances (Å) and X–M–Y angles (°): Cu–N(1) = 1.974(6); Cu–N(4) = 1.956(6); Cu–N(2) = 2.060(7); Cu–N(3) = 2.044(7); Cu–O(2) = 2.642(6); Cu–O(4) = 2.478(6); Cu–Cu = 7.887(2); N(1)–Cu–N(2) = 82.8(3); N(2)–Cu–N(3) = 87.0(3); N(3)–Cu–N(4) = 83.4(3); N(1)–Cu–N(4) = 109.3(2); N(2)–Cu–O(2) = 72.2(2); N(3)–Cu–O(4) = 77.0(3); O(2)–Cu–O(4) = 148.9(2).

3.3. X-ray structure of $[Cu_2(LtmpdH_{-4})]^{4-}$

Single crystals of the Cu^{2+} complex with $(Ltmpd)H_4$ were obtained from a strong basic solution. The X-ray structure shown in Fig. 7 indicates the formation of a binuclear chelate formulated as $[Cu_2(LtmpdH_{-4})]^{4-}$ in which four amide nitrogen atoms are deprotonated. Each metal ion is coordinated to two deprotonated amide nitrogen atoms and two amino nitrogen atoms, as schematically shown by Structure **B** in Fig. 1. The resulting coordination geometry is a square planar with a small tetrahedral distortion: four coordinated N atoms deviate only by ≈ 0.2 Å from the least-squares plane of CuN_4. The axial positions are occupied by carboxylate oxygen atoms with very long Cu–O distances (selected bond distances and bond angles are given in the figure caption). Each CuN_4 plane makes a dihedral angle of 78.9(2)° with respect to the *p*-phenylene ring plane, and two *p*-phenylene groups are stacked in a face-to-face manner. Amide nitrogen atoms N(1) and N(4) that are coordinated to the same metal ion are as close as 3.205(8) Å, which is much shorter than the interplane distance permissible for tetramethylphenylene groups that face each other; the van der Waals radius is 1.7 Å for aromatic carbon atoms and 2.0 Å for methyl groups [14]. For this reason, the amide nitrogen atoms deviate from the *p*-phenylene ring plane. In addition, the *para*-carbon atoms bonded to the amide nitrogen atoms are also forced to deviate from the *p*-phenylene ring plane toward the inside of the macrocyclic cavity (Table 2), resulting in the distortion of the *p*-phenylene ring in a boat form with a dihedral angle of 3.7–3.9°. The interatomic distance between the *para*-carbon atoms that face each other, C(11)–C(14)′, is 3.359(10) Å, which is still shorter than the van der Waals contact of carbon atoms, but, as a result of the distortion in the boat form, other four ring carbon atoms have looser interannular contacts: C(12)–C(15)′ = 3.452(10), C(13)–C(16)′ = 3.448(10) Å; the interplane distance is shown in Table 2. The distortion of a benzene ring in a boat form has been reported for alkyl[*n*]paracyclophanes and dialkyl[*n.n*]-paracyclophanes with short bridging chains [18–22]. Even for cyclophanes with a moderate chain length ($n = 8–12$), distortion in a boat is still significant as shown by X-ray studies and ab initio calculations: for example, the dihedral angle is 9° in [8]paracyclophane, 5° in [12]paracyclophane and 3.7° in 3,10-dioxo-2,5,8,11-tetraaza[12]paracyclophane [23–25]. The X-ray structure of $[Cu_2(LtmpdH_{-4})]^{4-}$ has shown that the N–Cu–N coordination bonds are strong enough to deform the π-electron ring, like the $(-CH_2-)_n$ bridges in [*n*]- and [*n.n*]paracyclophanes. Since the van der Waals radius of a methyl group is larger than that of a carbon atom, the interatomic distance of a pair of

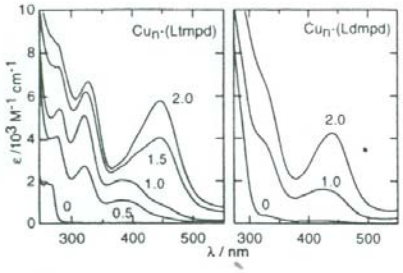

Fig. 8. UV and near-UV spectra of Cu^{2+} chelates with $(Ltmpd)^{4-}$ (left) in the ratio [Cu]/[L] = 0, 0.5, 1.0, 1.5 and 2.0 at pH 12; the spectra of Cu^{2+}–$(Ldmpd)^{4-}$ (right) in the ratio [Cu]/[L] = 0, 1.0 and 2.0 at pH 12. The molar absorptivity is given for each ligand molecule.

methyl carbon atoms facing each other should be longer than that of the ring-carbon pair: in fact, C(17)–C(19)′ = 3.581(13) and C(18)–C(20)′ = 3.655(13) Å. Consequently, the methyl carbon atoms deviate opposite to the direction in which the *para*-carbon atoms deviate: four methyl groups deviate to the same side, in contrast to the uncoordinated ligand in which the deviation of the methyl carbon atoms is irregular (Table 2). The distortion of the tetramethyl-*p*-phenylene ring is a result of the contraction of the highly constrained ligand molecule upon metal complexation.

3.4. Electronic absorption spectra of Cu^{2+} complexes

The X-ray study of $[Cu_2(\mathbf{L}tmpdH_{-4})]^{4-}$ has shown that the formation of the binuclear chelate results in severe steric constraints of the coordinated ligand molecule. This structural property influences the metal–ligand charge-transfer interaction and consequently metal–ligand charge-transfer bands in the near UV region of the absorption spectrum. A solution of a Cu^{2+}–$(\mathbf{L}tmpd)H_4$ mixture in the molar ratio [Cu]/[L] = 2 showed strong charge-transfer bands as shown in Fig. 8, in addition to a d–d band at 650 nm (log ∈ ($M^{-1}\,cm^{-1}$) ≈ 2.7 per Cu) at pH 12. At pH < 7, the charge-transfer bands weakened rapidly with decreasing pH: for example, the absorbance of the 450 nm band at pH 3 is 40% of that at pH 12. Simultaneously, the d–d band weakened and shifted to a longer wavelength; $\lambda_{max} \approx 680$ and log ∈ 1.9 at pH 3. This spectral change suggests the occurrence of interconversion between Structure **A** formed in acidic solutions and Structure **B** formed in basic solutions: in Structure **B**, the amide nitrogen atoms are coordinated to the metal ion, as shown by the X-ray study, and charge-transfer bands via the $Cu–N_{amide}$ bonds appear in the electronic spectra of basic solutions; in Structure **A**, the coordination of the amide oxygen atoms inhibits metal–ligand interaction, and the charge-transfer bands are absent in the electronic spectra of acidic solutions. In $[Cu_2(\mathbf{L}pdH_{-4})]^{4-}$ the absence of methyl groups makes it possible for two *p*-phenylene groups to be close to the van der Waals contact, 3.4 Å, without a severe distortion of the groups. The distortion of *p*-phenylene groups is, therefore, pronounced in the complex of the tetramethyl derivative. In fact, the spectral pattern observed for $[Cu_2(\mathbf{L}tmpdH_{-4})]^{4-}$ in the near UV region is more complicated than that observed for $[Cu_2(\mathbf{L}pdH_{-4})]^{4-}$; the spectrum of the latter complex is similar to that of $[Cu_2(\mathbf{L}dmpdH_{-4})]^{4-}$, which exhibits a single charge-transfer band at 440 nm as shown in Fig. 8.

In the solution spectra of Cu–$(\mathbf{L}tmpd)H_4$ mixtures with [Cu]/[L] ≤ 1 at pH 12, the 450 nm band disappeared and a new band was observed at 385 nm (Fig. 8). On the other hand, the 440 nm band of Cu_n–$(\mathbf{L}dmpd)H_4$ was not shifted with [Cu]/[L] ratio, although the band was intensified with increasing Cu^{2+} concentration (Fig. 8). The latter type of spectral change with [Cu]/[L] ratio has been commonly reported for the Cu^{2+} complexes of $(\mathbf{L}pd)H_4$ and other related macrocycles [9,10]. The less common spectral change observed for the Cu_n–$(\mathbf{L}tmpd)H_4$ system can be interpreted by assuming that: (1) the metal–ligand interaction in the CuN_4 units of the binuclear chelate molecule is different from that in the mononuclear chelate; (2) solutions with [Cu]/[L] ≤ 1 contain only the mononuclear species, and the binuclear species forms only when [Cu] > [L]. Since amide nitrogen atoms are deprotonated only when coordinated to a metal ion, the mononuclear metal chelate is formulated as $[Cu(\mathbf{L}tmpdH_{-2})]^{4-}$. The presence of the uncoordinated center in this mononuclear complex makes the ligand molecule less strained than that in the binuclear complex. Since the degree of the ligand distortion is different between the mononuclear and the binuclear chelates, assumption 1 is rational. Since the strain energy in the binuclear chelate is larger than that in the mononuclear chelate, the addition of a metal ion to the uncoordinated center in the mononuclear chelate requires a much higher energy than that for the formation of the mononuclear chelate, and hence assumption 2 is reasonable. Thus, the unusual spectral change with [Cu]/[L] ratio is a result of the ring contraction of the sterically constrained ligand molecule upon formation of the binuclear chelate.

4. Conclusions

The steric effect between methyl substituents and amide groups in $(\mathbf{L}tmpd)H_4$ defines the molecular dynamics that is observed in ^1H NMR spectra, and governs even the basicity of the amino nitrogen although the electron densities on the donor atoms are

not directly influenced. In the binuclear Cu^{2+} chelate of the macrocycle, the ligand molecule is distorted as a result of the ring contraction. The resulting strain energy leads to spectroscopic properties differing from those of the mononuclear Cu^{2+} chelate. This is a good example for preorganization of macrocyclic ligands, in which the coordination properties are governed by the steric effect without the electron densities on the donor atoms being changed.

5. Supplementary material

Crystallographic data for the structural analysis has been deposited with the Cambridge Crystallographic Data Centre, CCDC No. 155764 for compound Li_2H_2(Ltmpd)·$10H_2O$, CCDC No. 155765 for compound 3(Lpd)H_4·2HCl·$24H_2O$, and CCDC No. 155766 for compound $K_4[Cu_2(LtmpdH_{-4})]$·$11H_2O$. Copies of this information may be obtained free of charge from The Director, CCDC, 12 Union Road, Cambridge, CB2 1EZ, UK (fax: +44-1223-336033; e-mail: deposit@ccdc.cam.ac.uk or www:http://www.ccdc.cam.ac.uk).

Acknowledgements

The X-ray studies were carried out by using an X-ray diffractometer provided by the National Science Foundation (Grant No. CHE9610374) to the Molecular Structure Laboratory at the University of Arizona.

References

[1] E. Weber, in: J.L. Atwood, J.E.D. Davies, D.D. MacNicol (Eds.), Inclusion Compounds, vol. 4, Oxford University Press, New York, 1991, p. 188.
[2] F. Ebmeyer, F. Vögtle, in: J.L. Atwood, J.E.D. Davies, D.D. MacNicol (Eds.), Inclusion Compounds, vol. 4, Oxford University Press, New York, 1991, p. 263.
[3] T.W. Bell, S.K. Sahni, in: J.L. Atwood, J.E.D. Davies, D.D. MacNicol (Eds.), Inclusion Compounds, vol. 4, Oxford University Press, New York, 1991, p. 325.
[4] R.M. Izatt, K. Pawlak, J.S. Bradshaw, R.L. Breuning, Chem. Rev. 95 (1995) 2529.
[5] G.W. Gokel (Ed.), Molecular Recognition: Receptor for Cationic Guests (Comprehensive Supramolecular Chemistry), vol. 1, Pergamon/Elsevier Science, New York, 1996.
[6] V.L. Pecoraro, A.J. Stemmler, B.R. Gibney, J.J. Bodwin, H. Wang, J.W. Kampf, A. Barwinski, in: K.D. Karlin (Ed.), Progress in Inorganic Chemistry, vol. 45, Interscience/Wiley, New York, 1997, p. 83.
[7] J. Nelson, V. McKee, G. Morgan, in: K.D. Karlin (Ed.), Progress in Inorganic Chemistry, vol. 47, Interscience/Wiley, New York, 1998, p. 167.
[8] M.B. Inoue, E.F. Velazquez, M. Inoue, Q. Fernando, J. Chem. Soc., Perkin Trans. 2 (1997) 2113.
[9] M.B. Inoue, F. Medrano, M. Inoue, A. Raitsimring, Q. Fernando, Inorg. Chem. 36 (1997) 2335.
[10] M.B. Inoue, E.F. Velazquez, F. Medrano, K.L. Ochoa, J.C. Galvez, M. Inoue, Q. Fernando, Inorg. Chem. 37 (1998) 4070.
[11] M.B. Inoue, I.C. Muñoz, L. Machi, M. Inoue, Q. Fernando, Inorg. Chim. Acta 311 (2000) 50.
[12] K. Mikkelsen, S.O. Nielsen, J. Phys. Chem. 64 (1960) 632.
[13] A.K. Covington, M. Paabo, R.A. Robinson, R.G. Bates, Anal. Chem. 40 (1968) 700.
[14] L. Pauling, The Nature of the Chemical Bonds, 3rd ed., Cornell University Press, Ithaca, NY, 1960, p. 261.
[15] C.A. Hunter, J.K.M. Sanders, J. Am. Chem. Soc. 112 (1990) 5525.
[16] J.L. Sudmeier, C.N. Reiley, Anal. Chem. 36 (1964) 1699.
[17] M.B. Inoue, P. Oram, M. Inoue, Q. Fernando, Inorg. Chim. Acta 232 (1995) 91.
[18] C.J. Brown, J. Chem. Soc. (1953) 3265.
[19] C. Krieger, J. Liebe, W. Tochtermann, Tetrahedron Lett. 24 (1983) 707.
[20] J.E. Rice, T.J. Lee, R.B. Remington, W.D. Allen, D.A. Clabo Jr., H.F. Schaefer III, J. Am. Chem. Soc. 109 (1987) 2902.
[21] T. Tsuji, S. Nishida, J. Am. Chem. Soc. 110 (1988) 2157.
[22] S. Grim, J. Am. Chem. Soc. 114 (1992) 10542.
[23] M.G. Newton, T.J. Walter, N.L. Allinger, J. Am. Chem. Soc. 95 (1973) 5652.
[24] N.L. Allinger, L.A. Freiberg, R.B. Hermann, M.A. Miller, J. Am. Chem. Soc. 85 (1963) 1171.
[25] M.B. Inoue, F. Medrano, M. Inoue, Q. Fernando, J. Chem. Soc., Perkin Trans. 2 (1998) 2275.